ELSEVIER

Chemical Engineering Journal 133 (2007) 301–309

Chemical Engineering Journal

www.elsevier.com/locate/cej

Experimental investigation on aggregation of coal-fired PM_{10} by magnetic seeding

Changsui Zhao*, Yongwang Li, Xin Wu, Duanfeng Lu, Song Han

Key Laboratory of Clean Coal Power Generation and Combustion Technology of Ministry of Education, Southeast University, Nanjing 210096, PR China

Received 25 October 2006; received in revised form 13 February 2007; accepted 21 February 2007

Abstract

Particle aggregation by magnetic seeding was proposed for removing the coal-fired PM_{10}. To better understand the particle aggregation properties by magnetic seeding, experiments on the fly ash particles in the size range of 0.023–9.314 μm were conducted in a uniform magnetic field by seeding magnetic particles of Fe_3O_4 and γ-Fe_2O_3. The fly ash particles were produced from combustion of bituminous coal originated in Dongshen, China. A dedicated fluidized bed aerosol generator was developed to disperse particles to generate aerosol at a constant rate. The fly ash particles mixed with magnetic seed particles, underwent agglomeration during passing through the magnetic field. The variation in particles number concentration induced by aggregation was measured in real time by an electrical low pressure impactor. Characteristics of particles aggregation by seeding the two kinds of magnetic particles were examined. Experimental results show that particle removal efficiencies can be increased by increasing the magnetic flux density, the mass ratio of magnetic seed particles/fly ash and the particle residence time in the magnetic field. The removal efficiencies by seeding Fe_3O_4 are higher than those by seeding γ-Fe_2O_3 under the same conditions. When particles are saturatedly magnetized, further increasing the magnetic flux density no longer has effect on particle aggregation. Both the single-sized and total removal efficiencies of fly ash particles for seeding Fe_3O_4 are higher than those for seeding γ-Fe_2O_3. Mid-sized particles removal efficiencies are higher than those of the bigger ones or the smaller ones. Particle number median diameter decreases during aggregation, and the decrement for seeding Fe_3O_4 is lower than that for seeding γ-Fe_2O_3. Numerical simulation results indicated that particle removal efficiencies increase remarkably with the increase in total particle mass concentrations. The total removal efficiencies reach 84% and 62% for seeding Fe_3O_4 and γ-Fe_2O_3 respectively, and the particle number median diameter decrease from original 0.151 to 0.098 and 0.085 μm when total particle mass concentration is 40 g m^{-3}.

Keywords: Fine fly ash particles; Coal combustion; Aggregation; Magnetic seed particles; Removal efficiency

1. Introduction

PM_{10} has been concerned increasingly for its associating with increased mortality, morbidity and decreased lung function [1], especially emitted from coal combustion source in China [2,3]. The emission sources of PM_{10} such as coal-fired power plants contribute significantly to the ambient aerosol loading in the atmosphere [4]. Because of their tiny size, light weight and enormous number, conventional dust removal facilities are little effective on the fine fly ash particles from coal combustion. There are two ways to remove the fine fly ash particles from flue gas, one is to remove them with new-style facilities, and the other is to aggregate the particles first to enable the particles large enough, and then remove them with conventional facilities. Particle aggregation is the process of particle merging induced by their collision. Iron oxide is one of the main components constituting fly ash particle [5–7], so the particle can be magnetized easily in magnetic field [8]. In a magnetic field, the magnetized fly ash particles and magnetic seed particles come close and adhere together under the inter-particle magnetic dipole force and other primary forces such as drag, Brownian, van der Waals and gravity. Thus, aggregation of the fine fly ash particles by magnetic seeding in a magnetic field is a promising method of removing them from flue gas, and the project for investigating it was launched as one of the National Basic Research Programs of China.

The study on magnetic particle collision and aggregation has wide interest because of its applicability to many practical systems. Magnetic separation has been suggested as a recovery and pollution control process, such as for desulphurization of coal

* Corresponding author. Tel.: +86 25 83793453; fax: +86 25 83793453.
E-mail address: cszhao@seu.edu.cn (C. Zhao).

1385-8947/$ – see front matter © 2007 Elsevier B.V. All rights reserved.
doi:10.1016/j.cej.2007.02.021

Nomenclature

B	magnetic flux density (T)
C	mass concentration of particles (kg m^{-3})
d_m	number median diameter (μm)
d_p	particle diameter (μm)
n	size distribution of particle (m^{-6})
R	mass ratio of magnetic seed particles over fly ash
t	residence time of particle in magnetic field (s)
u	gas flow velocity (m s^{-1})
v_{min}, v_{max}	minimum and maximum volume of particles existing in gas flow (m^3)

Greek letters

β	aggregation coefficient (m^3 s^{-1})
η_s	single-sized particle removal efficiency (%)
η_t	total particle removal efficiency removal efficiency (%)

[9], for effluent from steel mills [10], for separation and concentration of mining ores and waste [11] and for hybrid solid–liquid separation processes [12]. Aggregation of small dust grains also results in interesting structures of the aggregates such as single chains and inter-connected web-like structures [13]. Aggregation process could be used to enhance the removal efficiency of high-gradient magnetic separations [14,15]. Particle aggregation in magnetic field has also been used for delivering therapeutic drugs [16] and purifying drinking water [17].

There have been some investigations on the collision and aggregation of particles in magnetic field. Smoluchowski [18] investigated the aggregation of airborne particles in static gas medium, and developed the Brownian agglomeration model for evaluating the agglomeration coefficient between two interacting particles. Based on the Brownian agglomeration model, Svoboda [19] considered the flocculation of weakly magnetic quasi-colloidal particles in suspensions, using an inter-particle force potential that includes electrical double layer, van der Waals and magnetic force. Chin et al. [20] studied the flocculation kinetics of mixtures of magnetite and polystyrene in a stirred tank under turbulent shear flow conditions. The results showed that the flocculation rate can be enhanced by increasing the agitation speed. By making mathematical approximations, Prakash and Pratim [21] derived the expression of collision frequency function for particles whose dipoles are randomly oriented and aligned in magnetic fields, neglecting all but the magnetic dipole force potential. Tsouris and Scott [22] carried out flocculation experiments of paramagnetic particles under the influence of a strong magnetic field. They found that aggregation is strong dependence on particle size and on magnetic susceptibility.

Although extensive studies have been conducted on the aggregation of magnetic particles, most of the studies were dealing with magnetic particles with bigger sizes in liquid medium. The investigation on aggregation of fine fly ash particles in uniform magnetic field in our previous paper [23] indicated that removal efficiency of the fly ash particles was lower than desired due to low magnetization. However, the magnetization of magnetic seed particles is much higher than that of fly ash particles. Thus, magnetic seed particles can be used to aggregate fine fly ash particles to heighten the removal efficiency of fly ash particles. To better understand the aggregation properties of fine fly ash particles in uniform magnetic field by seeding magnetic particles, and to provide a solid basis for the application of the aggregation technology by external magnetic field, this paper presents aggregation experiments on fine fly ash particles in the size range of 0.023–9.314 μm in a uniform magnetic field by seeding magnetic particles. The effects of particle size, magnetic flux density, total particle mass concentration, mass ratio of magnetic seed particles/fly ash, average gas velocity and particle residence time in the magnetic field were examined.

2. Experiments

2.1. Lab scale setup and procedure

The particle aggregation experimental system is schematically shown in Fig. 1. It consists of two HEPA filters, two fluidized bed aerosol generators, a jar, an aggregating passage, an electromagnet and a measurement apparatus. One of the HEPA filters was used to filter the nitrogen flowing into the fluidized bed aerosol generator and the diluter; another was used to filter the aerosol coming from the polycarbonate tube placed between the two magnetic heads. The two aerosol generators were used to generate the aerosols of fly ash and magnetic seed particles, respectively. And the jar's capacity is 0.001 m^3, which is used to mix aerosol particles of fly ash and magnetic seed particles.

The fluidized bed aerosol generator [24], shown in Fig. 2, is a relative simple apparatus for deagglomerating and aerosolizing fly ash particles. It consists of a dense bed, coarse particles (bronze beads) mixed with a solid powder (fly ash in this case).

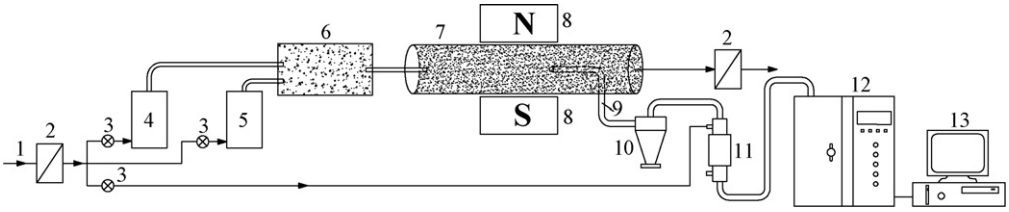

Fig. 1. Schematic diagram of experimental system. (1) Nitrogen gas; (2) HEPA filter; (3) flow meter; (4) fluidized bed aerosol generator for aerosolizing fly ash; (5) fluidized bed aerosol generator for aerosolizing magnetic seed particles; (6) aerosol mixing jar; (7) aggregating passage; (8) magnetic poles; (9) sampling probe; (10) cyclone; (11) Dekati diluter; (12) electrical low pressure impactor (ELPI); (13) external PC for data acquisition.

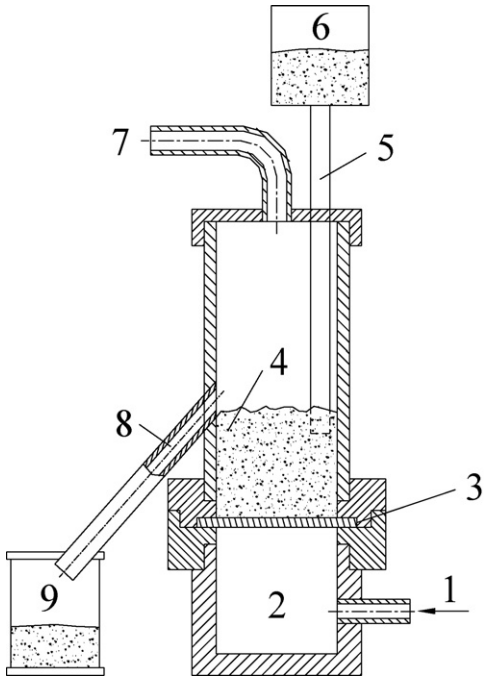

Fig. 2. The fluidized bed aerosol generator. (1) Nitrogen gas; (2) nitrogen plenum chamber; (3) distributor; (4) bed; (5) vertical tube; (6) fly ash/bronze reservoir; (7) aerosol outlet; (8) overflow outlet; (9) fly ash/bronze collector.

Nitrogen passing through the bed via the gas distributor fluidizes the bed. The bronze beads move and mix freely, grinding up the fly ash agglomerates. The smaller fly ash particles subsequently become entrained in the nitrogen flow, while the heavier bronze beads and the larger fly ash particles settle back to the bed. At the same time, the fresh bronze/fly ash mixture is added to the bed continuously through the vertical tube connected with the reservoir. In order to ensure that the bed maintains a relatively constant height, an overflow outlet is located at the higher part on the wall of the bed so that the excess mixture can be withdrawn continuously. The output of particle concentrations can be adjusted by changing the mass ratio of bronze beads/fly ash, the nitrogen flow rate through the bed, or the feed rate of the mixture.

An electromagnet (SB-100, China) generates a uniform magnetic field between its two magnetic heads. Diameter of both the magnetic heads is 100 mm, and the maximum magnetic flux density is 1.4 T. A transparent plexiglas tube, with an inside diameter of 50 mm, was placed between two magnetic heads as a passage for aerosol particles.

An electrical low pressure impactor (ELPI, Dekati Ltd., Finland) was employed to monitor particle size distribution and concentration in real time. The ELPI consists of 13 stages (12 channels), and the cut off diameter (D_{50}) of each stage and geometrical mean diameter (D_i) of each channel are shown in Table 1. Operating principle of the ELPI is based on inertial classification of electrically charged particles and the particle number is determined according to the electrical charge carried by different sized aerosol particles. To shield magnetic field so that the external magnetic field has no effect on the particles inside the sampling probe, a ferrite foil was adhibited on the surface of the sampling probe. The distance from the boundary of magnetic field to the sampling point can be changed by adjusting the position of the sampling probe along the axial direction of the polycarbonate tube. To remove particles larger than 9.314 μm from the sample gas flow, a cyclone was laid between the sampler and the Dekati dilutor. The dilutor enables sampling from high particle concentration over a long period of time. The dilutor has a constant dilution ratio of 8.18.

Fly ash particles and magnetic seed particles were aerosolized by the fluidized bed aerosol generators and came into the jar to mix fully. The mixed aerosol were transported into the plexiglas tube by gas flow and aggregated in magnetic field. The number concentrations of the fly ash particles both before and after aggregation were measured by the ELPI online.

2.2. Particles

One kind of fly ash particles and two kinds of magnetic seed particles were used in the study. The fly ash was sampled from the hopper of the fourth electrical field of electrostatic precipitators (ESP) for a tangential bituminous coal-fired utility boiler in Dalateqi Power Plant of China. The coal fired in the boiler is from Dongsheng, China. The two kinds of magnetic seed particles were γ-Fe_2O_3 and Fe_3O_4, respectively. Fig. 3 shows the particle size distributions measured by ELPI for the fly ash particles and magnetic seed particles aerosolized by the aerosol generators. Distinct difference among the fly ash particles and magnetic seed particles in size distribution can be seen. Fig. 4 illustrates the hysteresis loops of fly ash particles and magnetic seed particles. The hysteresis loops were measured by the Vibrating Sample Magnetometer (Lake Shore, 7400). At any given magnetic flux density, the magnetization of Fe_3O_4 is the highest, followed by γ-Fe_2O_3, and then fly ash.

Table 2 gives the rest of experimental conditions employed.

Table 1
Impactor properties

Impactor stage no.												
1	2	3	4	5	6	7	8	9	10	11	12	13
Aerodynamic $D_{50\%}$ (μm)												
0.023	0.030	0.050	0.098	0.211	0.317	0.576	0.891	1.505	2.243	3.758	6.285	9.314
Aerodynamic D_i (μm)												
0.026	0.039	0.070	0.144	0.259	0.427	0.716	1.158	1.837	2.903	4.860	7.651	

Table 2
Experimental conditions

Density of fly ash (kg m^{-3})	Density of Fe_3O_4 (kg m^{-3})	Density of γ-Fe_2O_3 (kg m^{-3})	Gas viscosity (Pa s)	Experimental temperature (K)
2200	4950	5180	1.83×10^{-5}	293 K

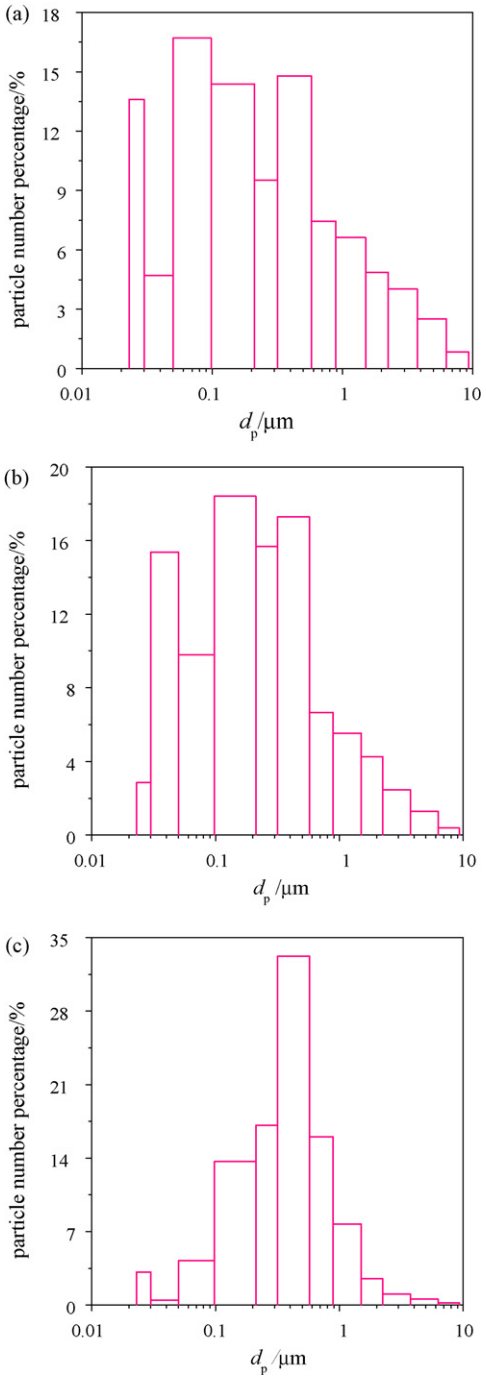

Fig. 3. Histograms of particle size distribution. (a) Fly ash particles, (b) magnetic seed particles of γ-Fe_2O_3 and (c) magnetic seed particles of Fe_3O_4.

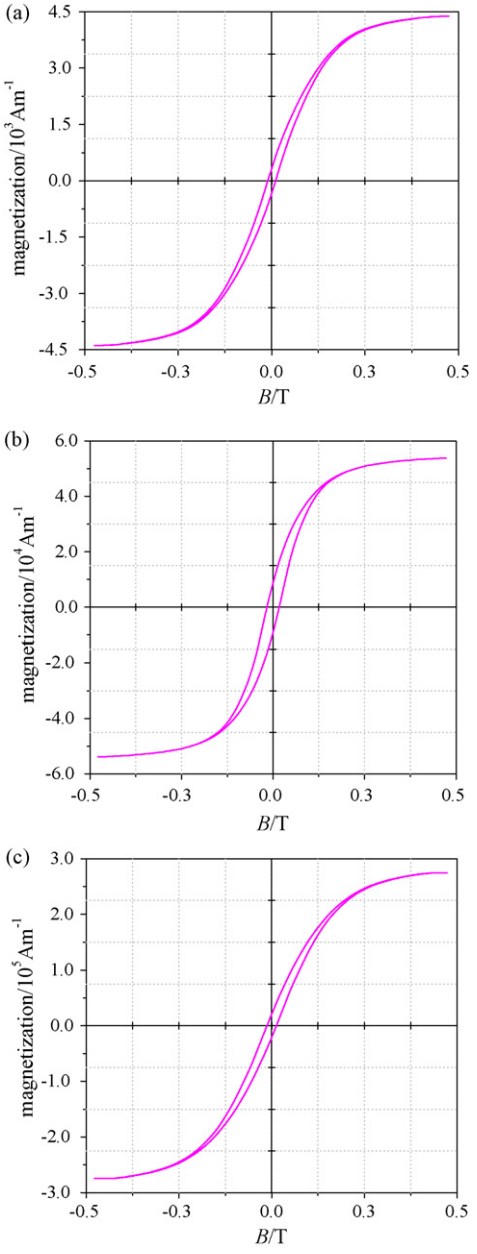

Fig. 4. Hysteresis loops of particles. (a) Fly ash particles, (b) magnetic seed particles of γ-Fe_2O_3 and (c) magnetic seed particles of Fe_3O_4.

3. Results and discussions

3.1. Particle aggregation mode

Aerosolized particles aggregate under the effect of the external magnetic field during passing through the aggregating passage. The resulting particles sampled at the outlet of the passage were observed by field emission scanning electron

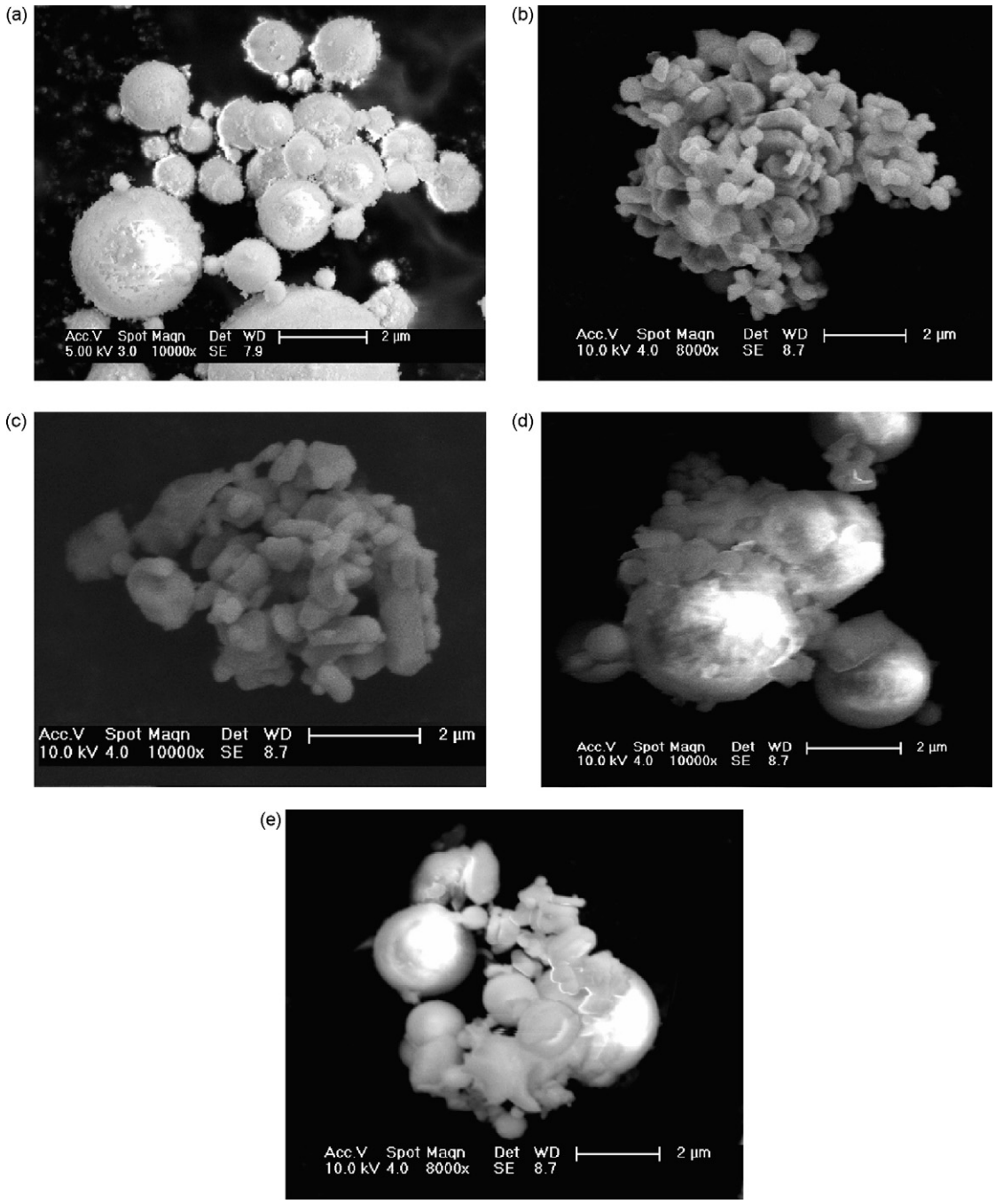

Fig. 5. SEM micrographs of aggregated particles. (a) Fly ash particles, (b) magnetic seed particles of γ-Fe_2O_3, (c) magnetic seed particles of Fe_3O_4, (d) fly ash particles seeding γ-Fe_2O_3 and (e) fly ash particles seeding Fe_3O_4.

microscope (Model FEI SIRION 200). Fig. 5 shows the SEM micrographs of the aggregates composed by fly ash particles, γ-Fe_2O_3, Fe_3O_4, fly ash particles seeding γ-Fe_2O_3 and fly ash particles seeding Fe_3O_4. It indicated that particles with different sizes aggregate together to compose bigger aggregates, and the aggregates composed by irregular γ-Fe_2O_3 and Fe_3O_4 are tighter than that those composed by spherical fly ash particles, shown in Fig. 5(a–c). For the aggregates of fly ash particles seeding γ-Fe_2O_3 and Fe_3O_4, the fly ash particles are connected by magnetic seed particles and aggregate tightly together, which is typical bridging aggregation [25] (Fig. 5(d and e)). Thus, it is a feasible way to aggregate fine fly ash particles by seeding magnetic particles.

3.2. Removal efficiency and number median diameter

Binary collision–aggregation is the dominating mode of particle aggregation, which results in variation of particle number concentration [26]. General dynamic equation (GDE) [27] can be used to predict the varying rate of particle number concen-

tration:

$$\frac{\partial n(v,t)}{\partial t} = \underbrace{\frac{1}{2}\int_{v_{\min}}^{v} \beta(u, v-u)n(u,t)n(v-u,t)\,\mathrm{d}u}_{\text{aggregation gain}} \underbrace{-n(v,t)\int_{v_{\min}}^{v_{\max}} \beta(u,v)n(u,t)\,\mathrm{d}u}_{\text{aggregation loss}} \quad (1)$$

where $\beta(u, v)$ is the aggregation coefficient (m^3/s) between two particles whose volumes are u and v. $n(v, t)$ is the size distribution function. $n(v, t)\,dv$ is the particle number concentration (particles per m^3) in the volume range v, $v + dv$ at time t. v_{min} is the volume for the smallest particles to occupy in the gas medium at time t, and v_{max} is the volume for the largest particles to occupy in the gas medium at the same time. The first term on the right-hand side of Eq. (1) represents the conversion rate of particles with volume u and volume $v - u$ into aggregates of volume v. The second term represents the conversion rate of particles of volume v to particles with larger size through collisions with particles of all sizes in the system.

During particle aggregating, the resulting particle aggregates larger than 9.314 μm will be removed by the cyclone before measurement. As a result of the aggregation, fly ash particle number concentration decreases. Single-sized particle removal efficiency (η_s) is the percentage of the decrease in number concentration of the certain sized particles over a certain time interval. Total particle removal efficiency (η_t) is the percentage of the decrease in total particle number concentration in the size range of 0.023–9.314 μm.

Eq. (1) indicates that particles aggregation coefficient and number concentrations are the main factors in their aggregation. The physical meaning of the aggregation coefficient is an effective collision volume between two interacting particles per unit time [28]. For magnetized particles, their aggregation coefficients increase with the increase in inter-particle forces. Thus, particle removal efficiency can be raised by increasing the inter-particle forces. Furthermore, higher particle number concentration also results in higher particle removal efficiency due to higher particle collision frequency.

Fig. 6 shows the effect of magnetic flux density on fly ash particle removal efficiency and number median diameter at total particle mass concentration C of 0.96 g m^{-3}, particle residence time in magnetic field t of 1.2 s, mass ratio of magnetic seed particles/fly ash R of 0.013 and gas flow velocity u of 0.08 m s^{-1}. Single-sized and total particle removal efficiencies rise as a result of the increase in magnetic flux density. This is because the magnetization of magnetic seed particles and fly ash particles increase with the increase in magnetic flux density before they attain saturation. The increase in magnetization results in the enhancement of inter-particle magnetic dipole force so that removal efficiencies rise. After particles magnetization becomes saturated, the further increase in magnetic flux density no longer has effect on particle aggregation. The magnetization of Fe_3O_4 is higher than that of γ-Fe_2O_3 under the same conditions, and the difference between them increases with the increase in magnetic

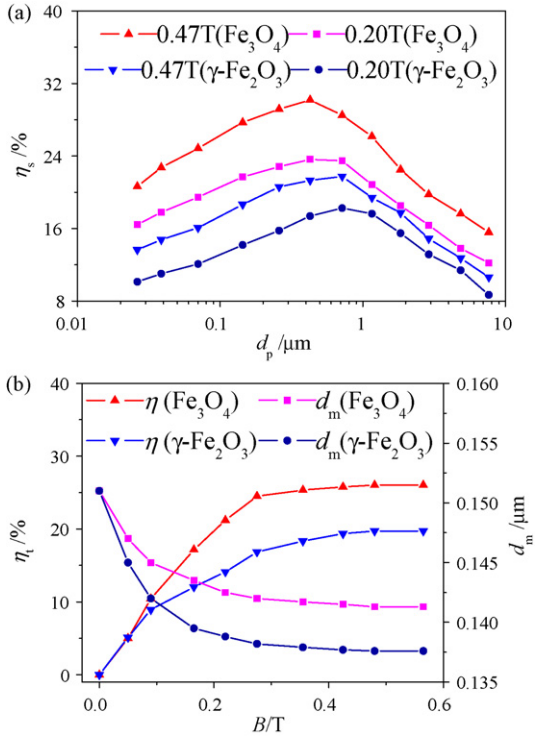

Fig. 6. Effect of magnetic flux density on fly ash particle aggregation at $C = 0.96$ g m^{-3}, $t = 1.2$ s, $R = 0.013$, $u = 0.08$ m s^{-1}. (a) Single-sized particle removal efficiency and (b) total particle removal efficiency and particle number median diameter.

flux density before saturatedly magnetized (Fig. 4). Therefore, under the same conditions, fly ash particle removal efficiency for seeding Fe_3O_4 are higher than that for seeding γ-Fe_2O_3, and their difference increases with the increase in magnetic flux density before particle magnetization attains saturation. For fly ash particles and magnetic seed particles with different size, both the inter-particles force and particle number concentration are different. Under the combined effect of aggregation coefficient and particle number concentration, removal efficiency of mid-sized particles are higher than that of the smaller or the bigger ones, and the particle size corresponding to the highest single-sized removal efficiency decreases slightly with the increase in magnetic flux density (Fig. 6(a)). Because removal efficiencies for different sized particle are different, the size distribution of fly ash particles varies continuously during aggregating, which can be evaluated by particle number median diameter d_m. d_m is commonly used to describe the particle size distribution, which means that 50% of the particles are smaller than d_m and 50% of the particles are bigger than d_m. Fig. 6(b) shows that particle number median diameter decreases with the increase in magnetic flux density and the decrement for seeding Fe_3O_4 is smaller than that for seeding γ-Fe_2O_3.

The mass ratio of magnetic seed particles over fly ash is another factor in particle aggregation. Higher mass ratio will result in higher collision frequency between the fly ash particles and the magnetic seed particles. Therefore, the fly ash particle removal efficiency can be increased by raising the mass ratio of magnetic seed particles over fly ash (Fig. 7). The increment in

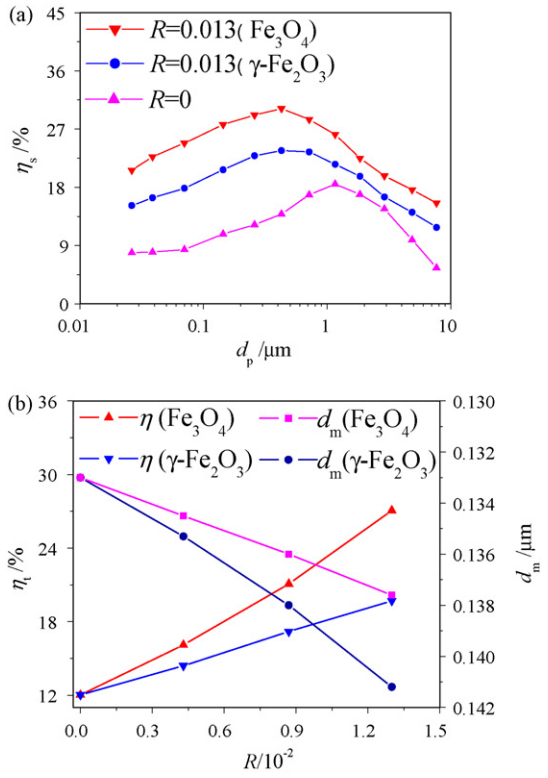

Fig. 7. Effect of mass ratio of magnetic seed particles over fly ash on fly ash particle aggregation at $B = 0.47$ T, $C = 0.96\ \mathrm{g\ m^{-3}}$, $t = 1.2$ s, $u = 0.08\ \mathrm{m\ s^{-1}}$. (a) Single-sized particle removal efficiency and (b) total particle removal efficiency and particle number median diameter.

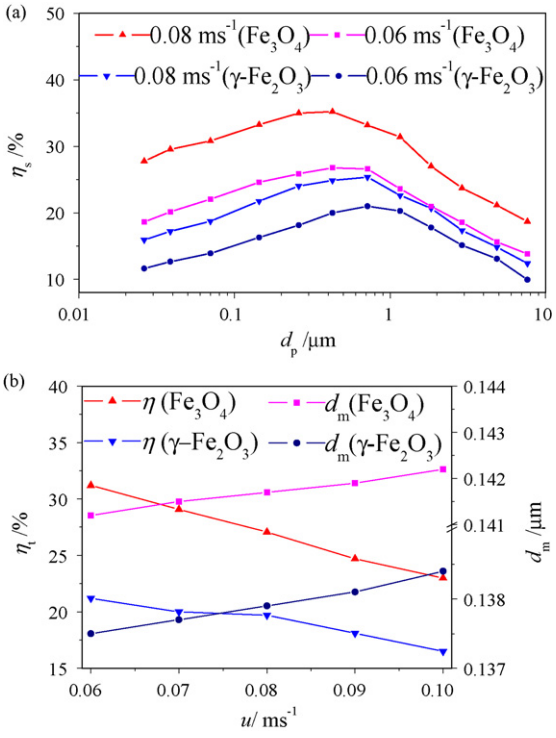

Fig. 8. Effect of gas flow velocity on fly ash particle aggregation at $B = 0.47$ T, $C = 0.96\ \mathrm{g\ m^{-3}}$, $R = 0.013$, $t = 1.0$ s. (a) Single-sized particle removal efficiency and (b) total particle removal efficiency and particle number median diameter.

removal efficiency for the smaller particles is higher than that for the bigger ones. Also, both the single-sized and total removal efficiencies for seeding Fe_3O_4 are higher than those for seeding γ-Fe_2O_3 under the same conditions. The particle number median diameter decreases with the increase in mass ratio, and the decrement for seeding Fe_3O_4 is smaller than that for seeding γ-Fe_2O_3.

Besides above factors, average gas velocity and particle residence time in the magnetic field affect the aggregation. Increasing average gas velocity will result in higher gas velocity gradient. Therefore, under the constant particle residence time in magnetic field, shear-induced aggregation will be intensified as the average gas velocity increases (Fig. 8) [20]. Prolonging particle residence time in the magnetic field, particle collision time rises. However, the physical dimension of the electromagnetic heads limits the maximum gas flow distance (equals $u \times t$) in the magnetic field. So the maximum particle residence time in the magnetic field decreases as the average gas velocity increases. Fig. 9 shows the effect of particle residence time on aggregation under the condition of maximum gas flow distance. It indicates that longer residence time in the magnetic field intensifies particle aggregation and increases particle removal efficiency. Moreover, Figs. 8 and 9 also indicate that the higher the total particle removal efficiency is, the smaller the particle size corresponding to the maximum particle removal efficiency is. The removal efficiency for seeding Fe_3O_4 is higher than that for seeding γ-Fe_2O_3 under the same conditions. Particle number median

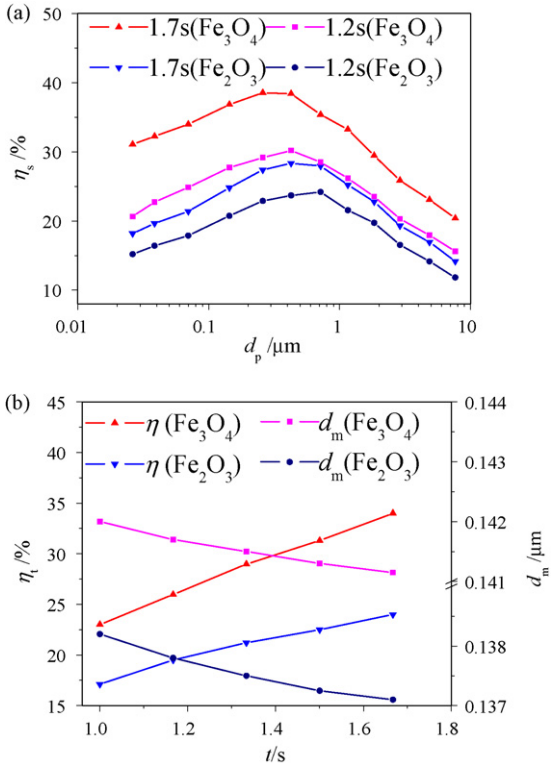

Fig. 9. Effect of particle residence time in magnetic field on fly ash particle aggregation at $B = 0.47$ T, $C = 0.96\ \mathrm{g\ m^{-3}}$, $R = 0.013$, $u \times t = 0.1$ m. (a) Single-sized particle removal efficiency and (b) total particle removal efficiency and particle number median diameter.

diameter decreases with the increase in residence time or average gas velocity, and the decrement for seeding Fe_3O_4 is lower than that for seeding γ-Fe_2O_3.

In practical dust removal systems, the mass concentrations of fly ash particles are much higher than those in this study. For the fly ash particles with higher mass concentration, the removal efficiency and number median diameter can be predicted by solving the general dynamic equation numerically.

4. Model prediction of particle removal efficiency

The particle size distribution can be measured by the ELPI. The binary collision-aggregation model [23] can be used to estimate the aggregation coefficient. When the particle size distribution and the aggregation coefficient are known, the general dynamic Eq. (1) can be solved by sectional method [29].

The single-sized and total particle removal efficiencies are predicted at $B = 0.47$ T, $R = 0.013$, $t = 1.2$ s, $u = 0.08$ m s^{-1}. It is found that the predicted removal efficiencies of fly ash particles are much higher in comparison with those of measurements in the experiments (Figs. 6–9). The total particle removal efficiencies increase remarkably as the total particle mass concentrations increase and they reach 84% and 63% for seeding Fe_3O_4 and γ-Fe_2O_3 when the total particle mass concentration is 40 g m^{-3}. Moreover, Fig. 10 shows that the particle number median diameter decreases more rapidly with the increase in total particle mass concentration compared with those of measured results shown in Figs. 6–9.

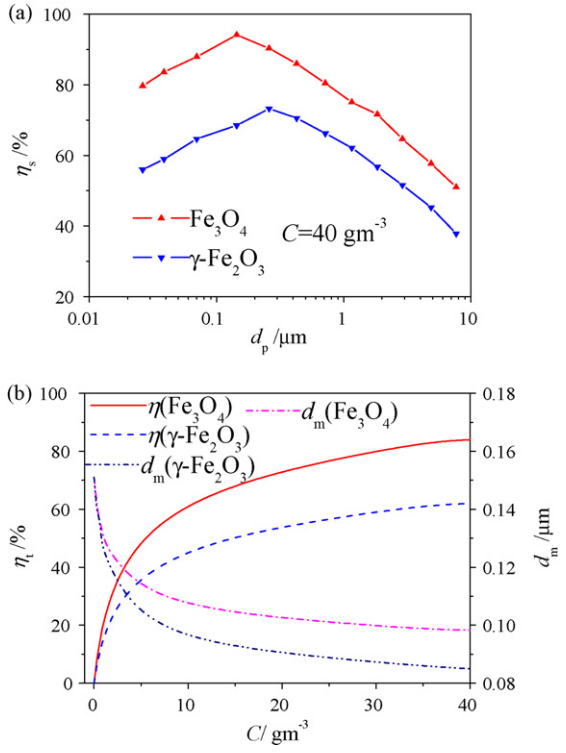

Fig. 10. Effect of particle mass concentration on fly ash particle aggregation at $B = 0.47$ T, $R = 0.013$, $t = 1.2$ s, $u = 0.08$ m s^{-1}. (a) Single-sized particle removal efficiency and (b) total particle removal efficiency and particle number median diameter.

It is evident that it is a more effective way to seed Fe_3O_4 than to seed γ-Fe_2O_3 for aggregating fly ash particles due to higher magnetization of Fe_3O_4 than that of γ-Fe_2O_3. Although increasing the magnetic flux density can intensify particle aggregation, further increase in the magnetic flux density has no effect after particles are saturatedly magnetized. Saturated magnetization of the particles can be reached at magnetic flux density more than 0.42 T, which can be easily realized by permanent magnet with smaller geometry than the electromagnet. Thus, for the same magnet geometry, especially designed permanent magnets enables a long particle residence time in magnetic field to increase removal efficiency. Also, permanent magnets are much cheaper in comparison with electromagnets and do not produce further energy cost. However, in this paper the electromagnet is used for better understanding the effect of magnetic flux density on particle aggregation. Higher mass ratio of magnetic seed particles over fly ash enables particle removal efficiency to increase, but it suffers higher operation cost at the same time. Therefore, it is desirable to aggregate particles by seeding magnetic particles with high magnetization in permanent magnet field for removing the coal-fired PM_{10}.

5. Conclusions

Submicron sized fly ash particle aggregation by magnetic seeding was shown to offer high potential in the field of coal-fired PM_{10} removing from flue gas. Due to inter-particle magnetic dipole force and other forces such as drag, Brownian, Van der Waals and gravity, fly ash particles come close and adhere together to form aggregates with bigger sizes so that they can be removed by conventional dust removal facilities. Experimental results indicated that removal efficiency of fly ash particles can be raised by increasing magnetic flux density, mass ratio of magnetic seed particles over fly ash, particle residence time in magnetic field. The increasing in the magnetic flux density no longer has effect on particle aggregation when particles are saturatedly magnetized. Both the single-sized and total removal efficiencies for seeding Fe_3O_4 are higher than those for seeding γ-Fe_2O_3. In the size range of 0.023–9.314 μm, removal efficiencies of mid-sized particles are higher than those of the bigger or the smaller ones. As a result of the aggregation, particle number median diameter decreases during aggregating, and the decrement for seeding Fe_3O_4 is smaller than that for seeding γ-Fe_2O_3. Predicted results demonstrated that particle removal efficiency increases remarkably with the increase in total particle mass concentration. The total removal efficiency reaches 84% and 62% for seeding Fe_3O_4 and γ-Fe_2O_3, respectively, and the particle number median diameter decreases from original 0.151 to 0.098 and 0.085 μm when particle mass concentration is 40 g m^{-3}.

In order to further increase the removal efficiency of submicron sized fly ash particles, seeding magnetic particles with high magnetization in permanent magnet field is suggested.

Acknowledgements

Financial support from the National Key Basic Research Program of China (No. 2002CB211600), Innovative Project

for Graduate Students in Universities of Jiangsu Province and Excellent Ph.D. Thesis of Southeast University were sincerely acknowledged. The authors also expressed sincere gratitude to Drs. Anthony and Leckner for presenting us valuable advices.

References

[1] P.E. Wagner, W.G. Kreyling, M. Semmler, et al., Health effects of ultrafine particles, J. Aerosol Sci. 35 (2004) 1155–1156.
[2] J.C. Sui, M.H. Xu, J.H. Qiu, et al., Formation and emission characteristic of PM_{10} at the coal-fired utility boiler, J. Eng. Thermophys. 27 (2006) 335–338.
[3] Y. Zhang, B. Zhao, Simulation and health risk assessment of residential particle pollution by coal combustion in China, Building Environ. 42 (2007) 614–622.
[4] Y.L. Jin, G.L. He, F. Liu, et al., Quantified study on human health impact caused by coal-burning air pollution in China, J. Hyg. Res. 31 (2002) 342–348.
[5] M.H. Fan, R.C. Brown, T.D. Wheelock, et al., Production of a complex coagulant from fly ash, Chem. Eng. J. 106 (2005) 269–277.
[6] X. Guo, C.G. Zheng, T. Sun, Physicochemical characteristics of fly ash from coal-fired power station, J. Combust. Sci. Technol. 11 (2005) 192–195.
[7] J.M. Sun, A study of the mineral composition of coal combustion results, Acta Mineral. Sinica 21 (2001) 14–18.
[8] Y.C. Zhao, J.Y. Zhang, Q. Gao, et al., Chemical composition and evolution mechanism of ferrospheres in fly ash from coal combustion, Proceedings of the Chinese Society of Electrical Engineering 26 (2006) 82–86.
[9] L. Petrakis, P.F. Ahner, F.E. Kiviat, Desulfurization and deashing of solvent refined coal by high gradient magnetic separation techniques, Sep. Sci. Technol. 16 (1981) 745–772.
[10] J. Svoboda, T. Fujita, Recent developments in magnetic methods of material separation, Miner. Eng. 16 (2003) 785–792.
[11] M.R. Parker, R.P.A.R.V. Kleef, H.W. Myron, et al., Kinetics of magnetic flocculation in colloidal dispersions, J. Colloid Interface Sci. 101 (1984) 314–319.
[12] M. Stolarski, B. Fuchs, S.B. Kassa, et al., Magnetic field enhanced press-filtration, Chem. Eng. Sci. 61 (2006) 6395–6403.
[13] H. Nübold, T. Poppe, M. Rost, Magnetic aggregation: II. Laboratory and microgravity experiments, Icarus 165 (2003) 195–214.
[14] A.T. Zimmer, P.A. Baron, P. Biswas, The influence of operating parameters on number-weighted aerosol size distribution generated from a gas metal arc welding process, J. Aerosol Sci. 33 (2002) 519–531.
[15] T.Y. Ying, S. Yiacoumi, C. Tsouris, High-gradient magnetically seeded filtration, Chem. Eng. Sci. 55 (2000) 1101–1113.
[16] Z.G. Forbes, B.B. Yellen, K.A. Barbee, et al., An approach to targeted drug delivery based on uniform magnetic fields, IEEE Trans. Magnet. 39 (2003) 3372–3377.
[17] S. Yiacoumi, D.A. Rountree, C. Tsouris, Mechanism of particle flocculation by magnetic seeding, J. Colloid Interface Sci. 184 (1996) 477–488.
[18] M. Smoluchowski, Versuch einer mathematischen Theorie der Koagulations-kinetik kolloider Löungen, Z. Phys. Chem. 92 (1917) 129–188.
[19] J. Svoboda, Magnetic flocculation and treatment of fine weakly magnetic minerals, IEEE Trans. Magnet. 18 (1982) 796–801.
[20] C.J. Chin, S. Yiacoumi, C. Tsouris, Shear-induced flocculation of colloidal particles in stirred tanks, J. Colloid Interface Sci. 206 (1998) 532–5454.
[21] K. Prakash, B. Pratim, Analytical expressions of the collision frequency function for aggregation of magnetic particles, J. Aerosol Sci. 36 (2005) 455–469.
[22] C. Tsouris, T.C. Scott, Flocculation of paramagnetic particles in a magnetic field, J. Colloid Interface Sci. 171 (1995) 319–330.
[23] Y.W. Li, C.S. Zhao, X. Wu, et al., Aggregation experiments on fine fly ash particles in uniform magnetic field, Powder Technology 174 (2007) 93–103.
[24] Y.W. Li, C.S. Zhao, X. Wu, et al., Development and characteristic of novel fluidized bed aerosol generator, J. Southeast Univ. 35 (2005) 742–745.
[25] S. Biggs, M. Habgood, G.J. Jameson, et al., Aggregate structures formed via a bridging flocculation mechanism, Chem. Eng. J. 80 (2000) 13–22.
[26] J. Zhao, J.W. Zhang, M. Xu, et al., Numerical study on particle size distribution in the process of preparing ultrafine particles by reactive precipitation, Chem. Eng. J. 110 (2005) 19–29.
[27] V.N. Piskunov, A.I.J. Golubev, C. Barrett, et al., The generalized approximation method for modeling coagulation kinetics-part 2: comparison with other methods, J. Aerosol Sci. 33 (2002) 65–75.
[28] Y. Koizumi, M. Kawamura, F. Tochikubo, et al., Estimation of the agglomeration coefficient of bipolar-charged aerosol particles, J. Electrostat. 48 (2000) 93–101.
[29] G. Yao, C.D. Sheng, L.J. Yang, et al., Spectrum evolution of combustion ultrafine particles acoustic agglomeration simulated by numerical algorithm, J. Combust. Sci. Technol. 11 (2005) 273–277.